Supplementary Information:

Dynamics of breaking intermolecular bonds in high-speed force spectroscopy

Manuel R. Uhlig, Carlos A. Amo, Ricardo Garcia*

Materials Science Factory
Instituto de Ciencia de Materiales de Madrid, CSIC
Sor Juana Inés de la Cruz, 28049 Madrid, Spain

*Correspondence to: r.garcia@csic.es

Materials and Methods

Tip Functionalization

The tip functionalization consists of two main steps. First, the silanization of the tips with APTES and, second, the subsequential functionalization with NHS-PEG27-biotin.

Chemicals. Phosphate buffered saline (PBS) powder, ethanol, 30% hydrogen peroxide, 1 N (0.5 mol/liter) sulfuric acid, 3-aminopropyltriethoxysilane (APTES) 99 %, trimethylamine ≥ 99 %, and avidin from egg white ≥ 98 % were purchased from Sigma-Aldrich (Madrid, Spain). The N-Hydroxysuccinimid (NHS)-polyethylenglycol (PEG27) - biotin linkers were purchased from JKU Linz.[1]

Silanization with APTES. Silicon nitride cantilevers (MSCT, Bruker, CA, USA) are cleaned thoroughly by immersing them in a piranha solution, a mixture of 0.5 N sulphuric acid and 30% hydrogen peroxide (4:1 ratio in volume) for 30 min. Then, the cantilevers are rinsed with ultrapure water and dried carefully using a flow of N_2. Hereafter, the cantilevers are immediately transferred into a 5 : 5 : 90 (vol :vol : vol) mixture of APTES : ultrapure water : ethanol to initiate the silanization of the tips. After 30 min, the cantilevers are rinsed with ethanol and ultrapure water and finally dried with N_2.

Functionalization with PEG-biotin. We dissolved 1 mg of the NHS-PEG27-Biotin linkers[1] in trichloromethane (0.5 ml). The obtained solution is transferred into a teflon chamber and 30 µl of tryethylamine are added as catalyst. Then, the silanized tips are immersed into the chamber. After an incubation time of 2 hours, the cantilevers are removed from the chamber, rinsed three times with trichloromethane, and dried with N_2.

Sample Preparation

The freeze-dried avidin is dissolved in 15 mM NaCl to obtain a solution with an avidin concentration of 0.1 mg/ml. Immediately afterwards, 33 µl of the solution are deposited on a freshly cleaved mica sheet. After 15 min of adsorption time, the mica is rinsed carefully 10 times with 1 mM NaCl and subsequently 3 times with 10 mM PBS.

AFM-based Single Molecule Force Spectroscopy

Single molecule force spectroscopy experiments were performed on a NanoWizard III AFM (JPK Instruments AG, Berlin, Germany). The entire experiment was carried out in 10 mM PBS at pH 7.4 at a temperature of T = 302 K.

A single rectangular silicon nitride cantilever (MSCT-B, Bruker, CA, USA) was used throughout the entire experiment. The cantilever's force constant k = 29 pN/nm, its resonance frequency f_0 = 3.05 kHz, and its quality factor Q = 1.6 were determined in PBS by fitting the thermal noise spectrum with the power spectral density of a damped single harmonic oscillator.[1] At the end of the experiment, the optical lever sensitivity S was calibrated by acquiring 100 deflection *versus* distance curves on a bare glass petri dish next to the mica substrate (S = 20 nm/V).

The SMFS curves were acquired by applying a periodic triangular modulation to the cantilever base with an amplitude of A_p = 250 nm. Fig. S1 illustrates the data acquisition protocol. First, the cantilever base is approached to the sample with a constant speed of 200 nm/s until a force of 150 pN is reached. This value was chosen to avoid the damage of the biotin. At this extension, the piezo is held for 20 ms. Then, the cantilever base is retracted with a constant pulling speed v_p. We have used pulling speeds in the 100 nm/s to 100 µm/s range. The piezo motion is shown in Fig. S1a for different pulling speeds. The piezo displacement was controlled using a calibrated closed-loop system. For each pulling speed value we have acquired between 100 and 600 individual SMFS curves with a spatial separation of 0.1 µm x 0.1 µm in between individual curves. The data sampling rate was adjusted for each speed value to keep the number of data points per piezo displacement distance constant.[2]

The AFM cantilever and the PEG linker represent a system of two springs in series. The effective spring constant of the cantilever-PEG system is equivalent to the slope of the retraction curves before the jump-off-contact. We obtain an average value of k_{eff} = 7.32 pN/nm which yields a linker stiffness of k_{PEG27} = 9.8 pN/nm and $k_{PEG27} = kk_{eff}/(k-k_{eff})$.

Loading rate

The loading rate has been determined in two ways. First, the loading rate r can be calculated by multiplying the effective force constant of the system with the pulling speed

$$r = k_{eff}\frac{d\psi}{dt} = k_{eff}v_p \qquad \text{(S1a)}$$

see eqn 4 (main text) and eqn S40, then for a triangular modulation $g_t = 2\tau/\tau_p$ where $\tau_p = 1/f_p$ is the period. The loading rate r for a triangular waveform is defined as

$$r = 2k_{eff}\frac{A_p f_0}{\varpi} = 2k_{eff}A_p f_p \qquad \text{(S1b)}$$

where A_p is the amplitude of the probe displacement during the force-distance curve, v_p the pulling speed and f_p the pulling frequency.

with $\varpi = f_0/f_p$ and f_0 is the resonant frequency of the cantilever. For a sinusoidal modulation $g_s(\omega_p,\tau) = \sin(\omega_p\tau)$

$$r = 2\pi k_{eff}\frac{A_p f_0}{\varpi} \qquad \text{(S1c)}$$

Alternatively, the effective loading rate can be obtained from the SMFS curves by fitting the force *versus* time data just before the unbinding event (Fig. S1c). Both approaches gave similar values (Fig. S2).

AFM-based SMFS Data Analysis

We have analysed 3100 force-distance curves by using a semi-automatic algorithm written in MATLAB (MathWorks, MA). The software fits the retraction part of the SMFS curves with a polynomial function of arbitrary grade. Then, the minima of the polynomial are determined and the algorithm searches in their vicinity for minima in the raw data. Minima with a force value smaller than the 1.5-fold of the baseline noise are disregarded. The unbinding events were selected by applying the general criteria of specific unbinding events (see ref. 25 in the main text). In addition, we have only considered events that showed characteristic lengths in the 7 to 25 nm range. Furthermore, in each curve only the last specific unbinding event is analysed to exclude the influence of multiple and spurious unbinding events. All the selected SMFS curves and the corresponding specific unbinding events can be individually displayed and visually inspected. A total of 846 curves showed features ascribed to specific unbinding events, i.e., a fraction of 25 %. This is in agreement with former avidin-biotin studies.[1,3]

Force spectroscopy measurements in liquid are affected by the hydrodynamic drag.[4,5] The associated force depends on the direction of the motion and value of the speed. It opposes the cantilever motion, so when the cantilever approaches it is repulsive and when the cantilever retracts it is attractive. Here, during the cantilever approach, the drag force is negligible due to the low approach speed. However, in the retraction part of the SMFS curve, the drag force can be significant.[5] Fig. S3a shows an example SMFS retraction curve obtained at a pulling speed of 10 μm/s. The drag force causes an effective attractive force that persists in the noncontact part of the curve (baseline). To remove this effect, we fit a linear function to the baseline of the retraction part (red line in Fig. S3a), subtract it from the raw data, and obtain the drag-free force curve (Fig. S3b). This correction is applied to every individual SMFS curve before we measure the unbinding force.

Approximation of the polymer extension

In the main text, Fig. 1b shows a freely joined chain (FJC) fit to the data.

$$d(F) = L_{\mathrm{C}}\left[\coth\left(\frac{Fl_{\mathrm{P}}}{k_{\mathrm{B}}T}\right) - \frac{k_{\mathrm{B}}T}{Fl_{\mathrm{P}}}\right] \tag{S2}$$

where L_C is the contour length, l_P the persistence length, k_B the Boltzmann constant, and T the absolute temperature. The fit yields L_C = 19.33 nm and l_P = 0.26 nm.

To find an analytical solution to eqn 4 the polymer extension has been approximated by using an exponential expression

$$F_{ts}(d,r) = \begin{cases} -F_{rup}(r)\dfrac{e^{\alpha d}-1}{e^{\alpha d_{rup}}-1}, & d \le d_{rup} \\ 0, & d > d_{rup} \end{cases} \approx \begin{cases} -F_{rup}(r)e^{\alpha\left(d-d_{rup}\right)}, & d \le d_{rup} \\ 0, & d > d_{rup} \end{cases} \tag{S3a}$$

where $F_{rup} = \dfrac{k_b T}{x_u}\ln\left(\dfrac{r x_u}{k_{off} k_B T}\right)$ is value of the unbinding force provided by the Bell–Evans force model. We consider that the force–distance curve is smooth enough close to the unbinding event to expand the force as

$$F_{ts}(d,r) \approx -F_{rup}(r)\left(1 + \alpha\left(d - d_{rup}\right) + \alpha^2/2\left(d - d_{rup}\right)^2 + \ldots\_ta \;\; consider\; the\; curve\; is\; sm\right.$$

(S3b)

α is a fitting parameter of the model with dimensions of L^{-1}. It is related to the effective force constant of the system and the bond length by $\alpha \approx k_{\mathrm{eff}}x_{\mathrm{u}}/k_{\mathrm{B}}T$; d_{rup} is the rupture distance of the linker:biotin-avidin system.

Fig. S4 shows a comparison between the FJC model and the exponential approximation. Near the unbinding event, the exponential approximation matches the experimental data and the FJC model. The fit parameters for eqn S16 are F_{unb} = 136 pN, α = 0.38 nm^{-1}, d_{rup} = 14.82 nm.

Analytical solution of the cantilever deflection during an unbinding event

The equation of motion (eqn 2 in the main text) is given by[6]

$$F_{ts}(\tau) = kz(\tau) + \frac{k}{Q\varpi}\frac{dz}{d\tau} + \frac{k}{\varpi^2}\frac{d^2z}{d\tau^2} \tag{S4}$$

where F_{ts} is the interaction force, k, Q are respectively the force constant and quality factor of the cantilever, $\varpi=f_0/f_p$ is the frequency ratio between the resonant and the modulation frequencies, z is the deflection and $\tau=\omega_p t$ is an adimensional time.

The general solution of Eq, S2 can be expressed in terms of the homogenous z_h and particular solutions z_p as

$$z(\tau) = z_h(\tau) + z_p(\tau) \tag{S5}$$

The solution for the homogenous equation

$$kz_h(\tau) + \frac{k}{Q\varpi}\frac{dz_h}{d\tau} + \frac{k}{\varpi^2}\frac{d^2z_h}{d\tau^2} = 0 \tag{S6}$$

with the initial conditions of

$$z_h(0) = 0;\ \frac{dz_h}{d\tau}(0) = z_0^{'} \tag{S7}$$

corresponds to the solution of a damped harmonic oscillator. In its most general form it is

$$z_h(\tau) = c_1 e^{\beta\varpi\tau} + c_2 e^{\beta^*\varpi\tau} \tag{S8a}$$

$$z_h^{'}(\tau) = c_1\varpi\beta e^{\beta\varpi\tau} + c_2\varpi\beta^* e^{\beta^*\varpi\tau} \tag{S8b}$$

where c_1 and c_2 are complex numbers and

$$\beta = \left(-\frac{1}{2Q} + i\sqrt{1-\frac{1}{4Q^2}}\right) \tag{S9}$$

By applying the initial conditions

$$z_h(0) = 0 = c_1 + c_2 \tag{S10a}$$

$$z_h^{'}(0) = c_1\varpi\beta + c_2\varpi\beta^* \tag{S10b}$$

we deduce that $c_1 = -c_2$ and

$$z_h^{'}(0) = z_0^{'} = c_1\varpi\left(-\frac{1}{2Q} + i\sqrt{1-\frac{1}{4Q^2}}\right) - c_1\varpi\left(-\frac{1}{2Q} - i\sqrt{1-\frac{1}{4Q^2}}\right) \tag{S11}$$

Frome those results

$$c_1 = -i\frac{z_0^{'}}{2\varpi q} = \frac{z_0^{'}}{2\varpi q}e^{-\frac{i\pi}{2}} = c_2^* \tag{S12}$$

with

$$q = \sqrt{1 - \frac{1}{4Q^2}} \tag{S13}$$

$$z_h^{'}(0) = c_1 + c_2^{*} = 2R(c_1) = 0 \tag{S14a}$$

$$z_h^{'}(0) = c_1\beta\varpi + c_1^{*}\beta^{*}\varpi = 2R(c_1\beta\varpi) = z_0^{'} \tag{S14b}$$

R defines the real part of a complex number. Then, the homogeneous solution is

$$z_h(\tau) = \frac{z_0^{'}}{q\varpi} e^{-\frac{\varpi\tau}{2Q}} \sin(\varpi\tau q) \tag{S15}$$

A particular solution of eqn S4 must satisfy

$$\frac{\varpi^2}{k} F_{ts}(\tau) = \frac{d^2 z_p}{d\tau^2} + \frac{\varpi dz_p}{Q\ d\tau} + \varpi^2 z_p(\tau) \tag{S16}$$

$$z_p(\tau) = c_1(\tau) e^{\beta\omega\tau} + c_2(\tau) e^{\beta^{*}\omega\tau} \tag{S17}$$

$$c_1(\tau) = -\frac{\varpi^2}{k} \int \frac{F_{ts}(\tau) e^{\beta^{*}\omega\tau}}{W\left[e^{\beta\varpi\tau}, e^{\beta^{*}\varpi\tau}\right](\tau)} d\tau \tag{S18a}$$

$$c_2(\tau) = \frac{\varpi^2}{k} \int \frac{F_{ts}(\tau) e^{\beta\omega\tau}}{W\left[e^{\beta\varpi\tau}, e^{\beta^{*}\varpi\tau}\right](\tau)} d\tau \tag{S18b}$$

where β^{*} is the complex conjugated of β and $W[f_1(x), f_2(x)](x)$ is the Wronskian of the functions $f_1(x), f_2(x)$, $W[f_1(x), f_2(x)] = f_1(df_2/dx) - f_2(df_1/dx)$,

$$c_1(\tau) = -\frac{i\varpi}{2kq} \int F_{ts}(\tau) e^{-\beta\omega\tau} d\tau \tag{S19a}$$

$$c_2(\tau) = \frac{i\varpi}{2kq} \int F_{ts}(\tau) e^{-\beta^{*}\omega\tau} d\tau \tag{S19b}$$

Then the general solution is given by

$$z(\tau) = \frac{z_0^{'}\sin(\varpi\tau q)}{\varpi \quad q} e^{-\frac{\varpi\tau}{2Q}} - \frac{ie^{\beta\varpi\tau}\varpi}{2q \quad k}\int F_{ts}(\tau)e^{-\beta\varpi\tau}d\tau + \frac{ie^{\beta\varpi\tau}\varpi}{2q \quad k}\int F_{ts}(\tau)e^{-\beta^{*}\varpi\tau}d\tau$$

(S20)

To obtain the deflection $z(\tau)$ at a given time τ_0 near the unbinding event as a function of the loading rate we introduce the following considerations. First, we neglect the contribution of homogeneous solution $z_h(\tau)$ to the rupture force because the it decays exponentially as exp(-$\varpi\tau_0/2Q$) (see eqn S20). Second, we determine the solution at the time at which the bond is broken $\tau=\tau_{rup}$

$$\lim_{\tau\to\tau_{rup}} z(\tau,\varpi) \approx \lim_{\tau\to\tau_{rup}} z_p(\tau,\varpi) = z_{rup}(\varpi) \qquad \text{(S21)}$$

Then from eqn S20 we deduce

$$\lim_{\tau\to\tau_{rup}} z_p(\tau,\varpi) = R\left(-\frac{i\beta}{qk}\sum_{n=0}^{\infty}\frac{F^{n)}(\tau_{rup})(-1)^n}{\varpi^n}e^{i\text{natan}\,2Qq}\right) \qquad \text{(S22)}$$

where we have used the following relationships

$$z_p(\tau) = -\frac{i\ \varpi}{2q\,k}\sum_{n=0}^{\infty}\frac{F^{n)}(\tau_{rup})(\tau-\tau_{rup})^n}{n! \qquad \varpi}e^{i\text{atan}\,2Qq}P_n\left(\frac{1}{\gamma(\tau-\tau_{rup})}\right) + cc = R\left(-\frac{i\varpi}{q\,k}\sum_{n=0}^{\infty}\frac{F^{n)}}{}\right.$$

(S23)

The force at times near τ_{rup} has been expressed in terms of a Taylor expansion as

$$F_{ts}(\tau) = \sum_{n=0}^{\infty}\frac{F^{n)}(\tau_{rup})}{n!}(\tau-\tau_{rup})^n \qquad \text{(S24)}$$

In addition we have used

$$(\tau-\tau_{rup})^n P_n = (\tau-\tau_{rup})^n + a_1\frac{(\tau-\tau_{rup})^{n-1}}{\gamma} + \ldots + a_n\frac{1}{\gamma^n} \qquad \text{(S25a)}$$

$$a_n = (-1)^n n! \qquad \text{(S25b)}$$

$$\gamma = \varpi e^{-i\text{atan}\,2Qq} \qquad \text{(S25c)}$$

$$F^{n)} = \frac{d^n F}{dd^n}\left(\frac{d\psi}{d\tau}\right)^n \quad \text{with } (d\psi/d\tau)=v_p \text{ assumed as constant and } >0 \qquad \text{(S25d)}$$

$$F^{n)}(d=d_{rup}) = -F_{rup}(r)\alpha^n \qquad \text{(S25e)}$$

In the above expressions we assume that distance is related to the time by (see also eqn 4 in the main text)

$$d(\tau) = z_c + z(\tau) + \psi(\tau) \approx z_c + \psi(\tau) \tag{S26}$$

The integrals included in eqn S20 has been solved by iteration using the following

$$\int x^n e^{\beta\varpi x} dx = \frac{x^n e^{\beta\varpi x}}{\beta\varpi}\left(1 - \frac{n}{x^n} e^{-\beta\varpi x} \int x^{n-1} e^{\beta\varpi x} dx\right) = \frac{x^n e^{\beta\varpi x}}{\beta\varpi} P_n\left(\frac{1}{\beta\varpi x}\right) \tag{S27a}$$

$$x = \tau - \tau_{rup} \tag{S27b}$$

where P_n is a polynomial of grade n in the variable $(1/x\beta\varpi)$ with coefficients $a_n = (-1)^n\, n!$.

Equation (S22) is limited by the interaction model. If we assume the interaction force near the unbinding event is given by eqn S3b, we obtain

$$\lim_{\tau \to \tau_{rup}} z_p(\tau, \varpi) = 2R\left(\frac{i}{2q} F_{rup}(r) \frac{q}{k} \sum_{n=0}^{\infty}\left(\frac{-\left(\frac{d\psi}{d\tau}\right)\alpha}{\varpi} e^{i\text{atan}\, 2Qq}\right)n\right) \tag{S28a}$$

$$z_{rup}(\varpi) = \lim_{\tau \to \tau_{rup}} z_p(\tau,\varpi) = \frac{\left(\frac{-F_{rup}}{k}\right)}{1 + \left(\frac{\left(\frac{d\psi}{d\tau}\right)\alpha}{\varpi}\right)^2 + \frac{\left(\frac{d\psi}{d\tau}\right)\alpha}{\varpi Q}} \tag{S28b}$$

To reach eqn S28b we have considered that the sum included in S28a is a geometric series with a common ratio $(d\psi/d\tau)\alpha/\varpi$. In general $(d\psi/d\tau) < \alpha/\varpi$ except for frequency ratios $\varpi \approx 1$. then

$$\sum_{n=0}^{\infty}\left(\frac{\left(\frac{d\psi}{d\tau}\right)\alpha}{\varpi} e^{i\text{atan}\, 2Qq}\right)n = \frac{1}{1 + \frac{\left(\frac{d\psi}{dt}\right)\alpha}{\varpi} e^{i\text{atan}\, 2Qq}} \tag{S29}$$

$$\frac{\left(\frac{d\psi}{dt}\right)\alpha}{\varpi} = \frac{v_p \alpha}{\varpi} < 1$$

The force measured in a SMFS is obtained by multiplying eqn S28b by the force constant of the cantilever

$$kz_{rup}(r) = F_m = \frac{-\frac{k_B T}{x_u}\ln\left(\frac{r x_u}{k_{off} k_B T}\right)}{1 + \left(\frac{r\alpha}{k_{eff} f_0}\right)^2 + \frac{r\alpha}{k_{eff} f_0 Q}} \tag{S30}$$

Then, we can obtain the value of the rupture force at any loading rate as

$$F^*_{rup} = F_m(r)N(r) = F_m(r)\left[1 + \left(\frac{r\alpha}{k_{eff} f_0}\right)^2 + \frac{r\alpha}{k_{eff} f_0 Q}\right] \tag{S31}$$

In our experiments, we have set the amplitude to A_p = 250 nm and α=0.03 nm^{-1} (obtained from Fig. 2) so our approximation is valid up to a frequency ratio ϖ =15 (χ = 222).

Asymptotic limit

The above expressions have the proper asymptotic limit for large frequency ratios. First, the homogenous solution vanishes for large values of ϖ,

$$|z_h(\tau)| \le \frac{z_0'}{\varpi} q\, e^{-\frac{\varpi\tau}{2Q}} \tag{S32}$$

consequently

$$\lim_{\varpi\to\infty} z(\tau) = \lim_{\varpi\to\infty} z_p(\tau) \tag{S33}$$

$$\begin{aligned}\lim_{\varpi\to\infty} z_p(\tau) &= 2R\left(-\frac{i\,\varpi}{2q\,k}\sum_{n=0}^{\infty}\frac{F^{n)}(\tau^*)(\tau-\tau^*)^n}{n!\qquad\varpi}e^{i\text{atan}\,2Qq}\right) = \frac{1\sin\,(\text{atan}\,2Qq)}{q\qquad k}\sum_{n=0}^{\infty}\frac{F^{n)}(\tau^*)}{n!}(\tau - \\ &= \frac{1}{k}\sum_{n=0}^{\infty}\frac{F^{n)}(\tau^*)}{n!}(\tau-\tau^*)^n\end{aligned} \tag{S34}$$

In the above, we have used the following identities

$$\sin\,(\text{atan}\,x) = x\left(1+x^2\right)^{-1/2} \tag{S35a}$$

$$\cos(\operatorname{atan} x) = \left(1 + x^2\right)^{-1/2} \tag{S35b}$$

$$\lim_{\varpi \to \infty} P_n(\tau) = 1 \;\forall\, n,\tau \tag{S35c}$$

eqn S34 is valid for any instant $\tau \neq \tau^*$, because τ^* is chosen in an arbitrary way.

The last term in eqn S34 is the Taylor expansion of the interaction force, in other words

$$\lim_{\varpi \to \infty} z_p(\tau) = \frac{1}{k}\sum_{n=0}^{\infty} \frac{F^{n)}(\tau^*)}{n!}(\tau - \tau^*)^n = \frac{1}{k}F_{ts}(\tau) \tag{S36}$$

which gives the Hooke's law

$$F_{ts}(\tau) = F_m(\tau) = kz_p(\tau) \tag{S37}$$

Appendix I. Space and time relationships

The instantaneous separation between the ligand and the receptor can be expressed by

$$d(\tau) = z_c + z(\tau) + \psi(\tau) \tag{S38a}$$

$$\psi(\tau) = A_p g(\omega,t) \tag{S38b}$$

where z_c is the mean tip–sample distance, $\psi(\tau)$ is the distance modulation applied to the z-piezo and $g(\omega t)$ is the type of waveform (sinusoidal, triangular,…). Then the force eqn S4 can be alternatively expressed as

$$F_{ts}(d) = kz(d) + \frac{kx_c}{Q}\chi\frac{dz}{dd} + kx_c^2\chi^2\frac{d^2z}{dd^2} \tag{S39}$$

with $x_c = 0.15\ nm$ the carbon-carbon distance in an amino acid chain and $\chi = v_p/x_c f_0$, where v_p is the pulling speed. χ is related to the frequency ratio $\varpi=\omega_0/\omega$ by $\chi = 2A_p/\varpi$ for a triangular modulation.

The deflection $z(\tau)$ is of the order of 0.1-1 nm while A_p=250 nm in these experiments. Consequently,

$$d(\tau) \approx z_c + \psi(\tau) \tag{S40}$$

Appendix II. **Induction proof of result (S11).**

For $n = 0$

$P_0 = 1$

$$\int x^n e^{\gamma x} dx$$

$$= \frac{x^n e^{\gamma x}}{\gamma}\left(1 - \frac{n}{x^n} e^{-\gamma x} \int x^{n-1} e^{\gamma x} dx\right) = \frac{x^n e^{\gamma x}}{\gamma}\left(1 - \frac{n}{x^n} e^{-\gamma x} \frac{x^{n-1}}{\gamma} e^{\gamma x}\left(1 - \frac{n}{x}\right.\right.$$

$$= \frac{x^n e^{\gamma x}}{\gamma}\left(1 - \frac{n}{x\gamma}\left(1 - \frac{n-1}{x^{n-1}} e^{-\gamma x} \int x^{n-2} e^{\gamma x} dx\right)\right)$$

$$P_n(\gamma x) = 1 - \frac{n}{x\gamma}\left(1 - \frac{n-1}{x^{n-1}} e^{-\gamma x} \int x^{n-2} e^{\gamma x} dx\right)$$

For $n+1$:

$$\int x^{n+1} e^{\gamma x} dx$$

$$= \frac{x^{n+1} e^{\gamma x}}{\gamma}\left(1 - \frac{n+1}{x^n} e^{-\gamma x} \int x^n e^{\gamma x} dx\right) = \frac{x^{n+1} e^{\gamma x}}{\gamma}\left(1 - \frac{n+1}{x^{n+1}} e^{-\gamma x} \frac{x^n e^{\gamma x}}{\gamma} P_n\left(\frac{1}{x\gamma}\right)\right)$$

$$= \frac{x^{n+1} e^{\gamma x}}{\gamma}\left(1 - \frac{n+1}{x^{n+1}} e^{-\gamma x} \frac{x^n e^{\gamma x}}{\gamma} P_n\left(\frac{1}{x\gamma}\right)\right)$$

$$= \frac{x^{n+1} e^{\gamma x}}{\gamma}\left(1 - \frac{n+1}{x\gamma} P_n\left(\frac{1}{x\gamma}\right)\right) = \frac{x^{n+1} e^{\gamma x}}{\gamma}\left(1 + S_1\left(\frac{1}{xy}\right) P_n\left(\frac{1}{x\gamma}\right)\right)$$

S_1 is a polynomial of grade 1 with no independent term $(a_0 = 0)$. Then,

$$S_1\left(\frac{1}{xy}\right) P_n\left(\frac{1}{x\gamma}\right) = S_{n+1}\left(\frac{1}{x\gamma}\right)$$

is a polynomial of grade $n+1$ with $a_0 = 0$ and

$$\int x^{n+1} e^{\gamma x} dx = \frac{x^{n+1} e^{\gamma x}}{\gamma}\left(1 + S_{n+1}\left(\frac{1}{x\gamma}\right)\right) = \frac{x^{n+1} e^{\gamma x}}{\gamma} P_{n+1}\left(\frac{1}{x\gamma}\right)$$

which by induction demonstrates the derivation of eqn S27a.

Supplemental Information figures

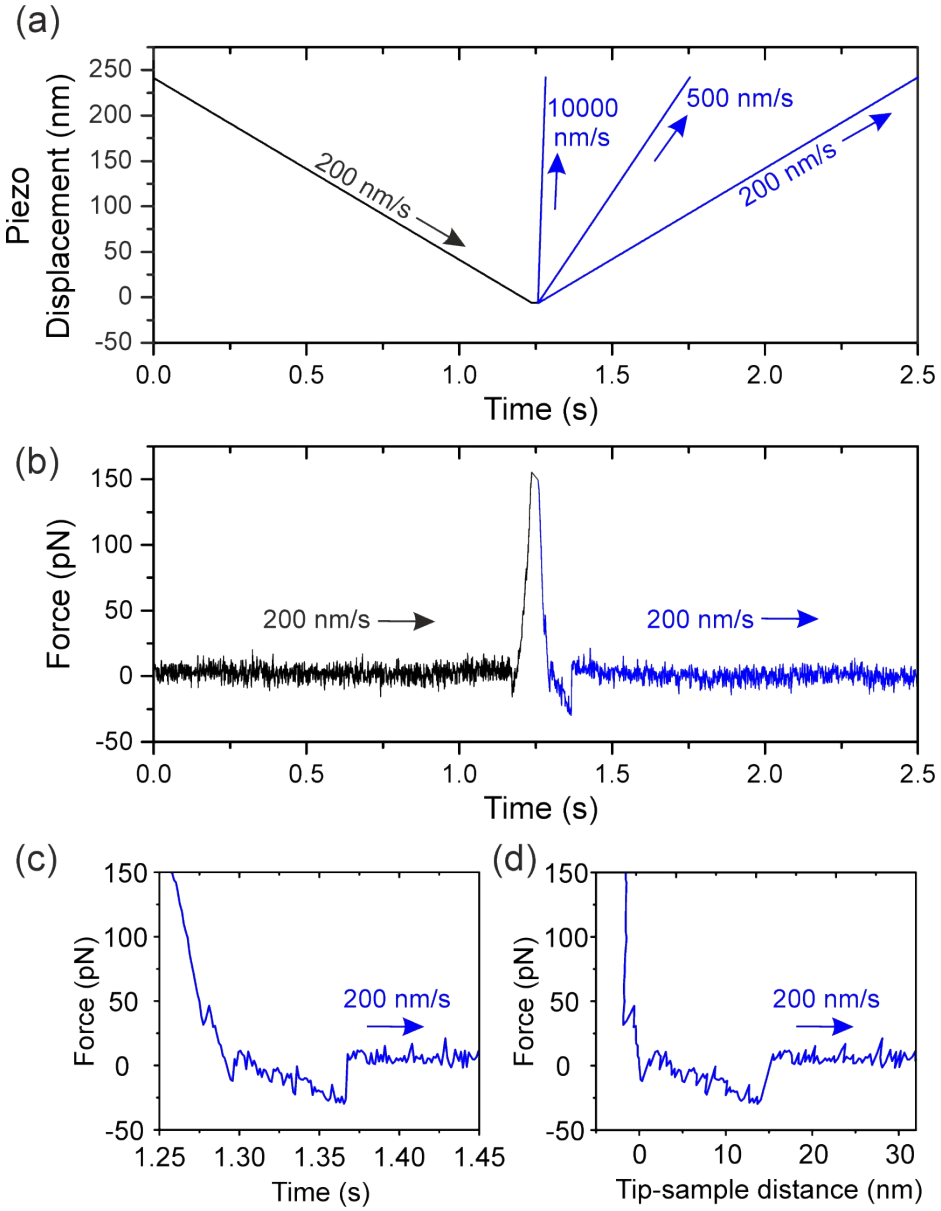

Figure S1. (a) The triangular modulation applied to the cantilever base for different pulling speeds. (b) Example of an SMFS curve obtained at a pulling speed of 200 nm/s. (c) Zoom-in into the force vs time curve around the unbinding event shown in (b). (d) The same force data as in (c), but plotted versus the tip-sample distance.

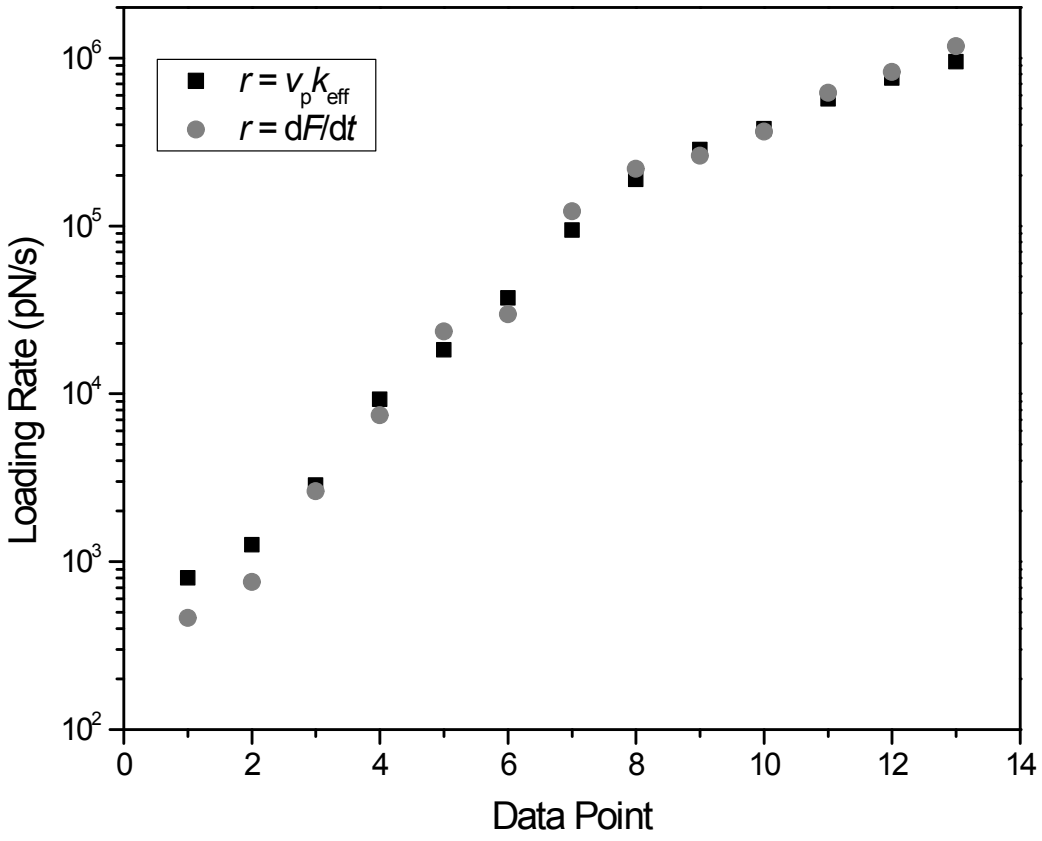

Figure S2. The loading rate has been determined in two ways. First, by multiplying the pulling speed with the effective force constant of the system, i.e. $r=v_p k_{eff}$ (in black), and, alternatively, by fitting the force *versus* time data just before the unbinding event (in grey).

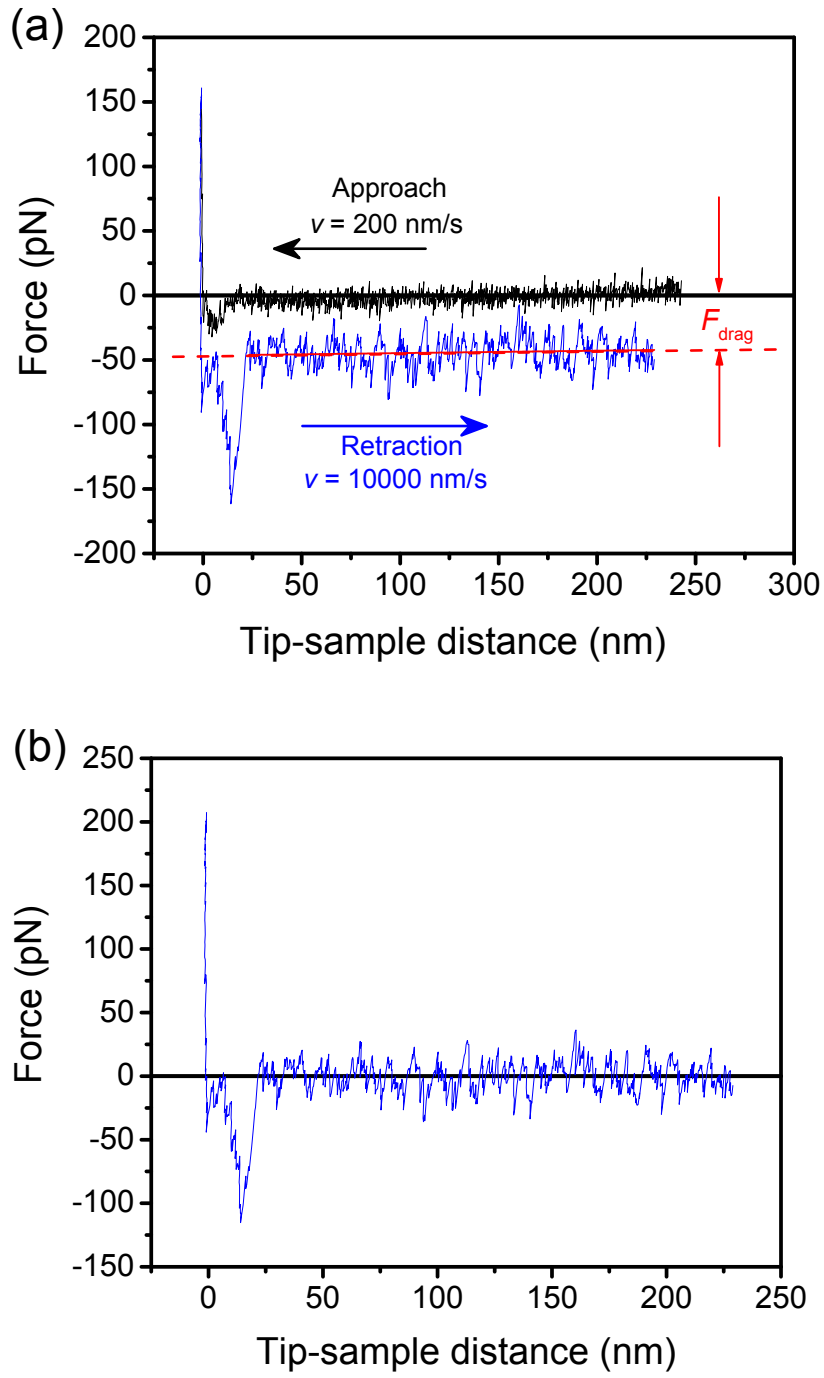

Figure S3. Example of an SMFS curve obtained at a pulling speed of 10 µm/s. (a) Raw data before applying the drag correction and (b) after the subtraction of the linear drag (approach curve omitted for clarity).

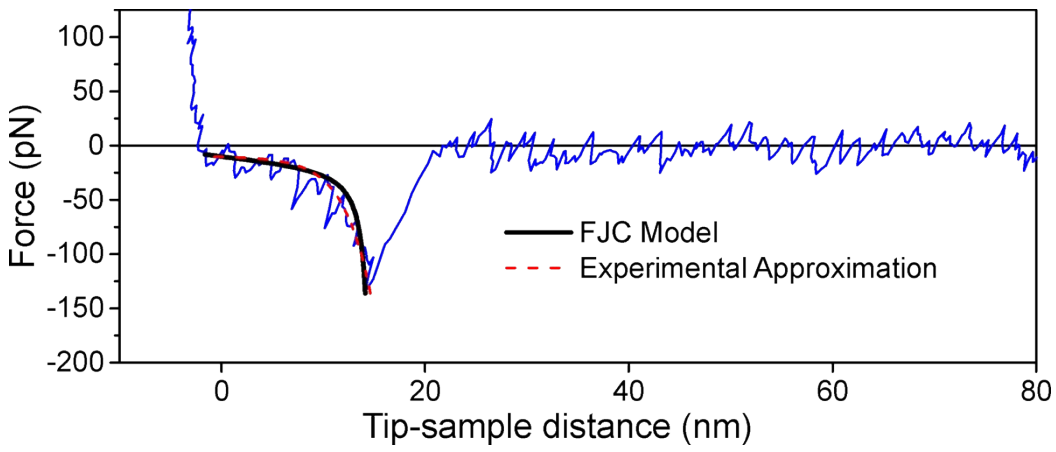

Figure S4. Comparison of the FJC polymer extension model and the exponential approximation. The AFM-based SMFS curve was obtained at a pulling speed of 4 μm/s. The data is the same as in Fig. 1b of the main text.

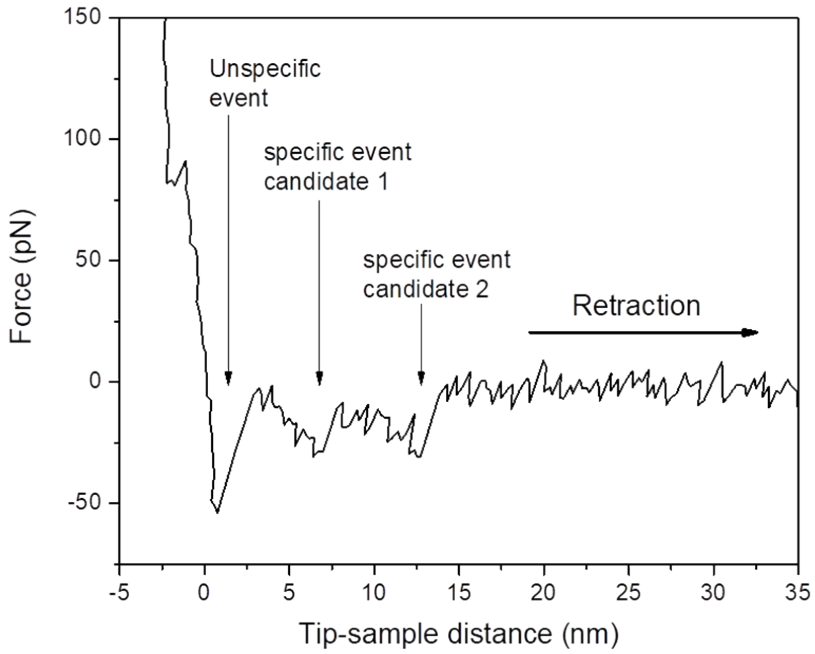

Figure S5. AFM-based SMFS curve that shows multiple unbinding events for the avidin-biotin system.

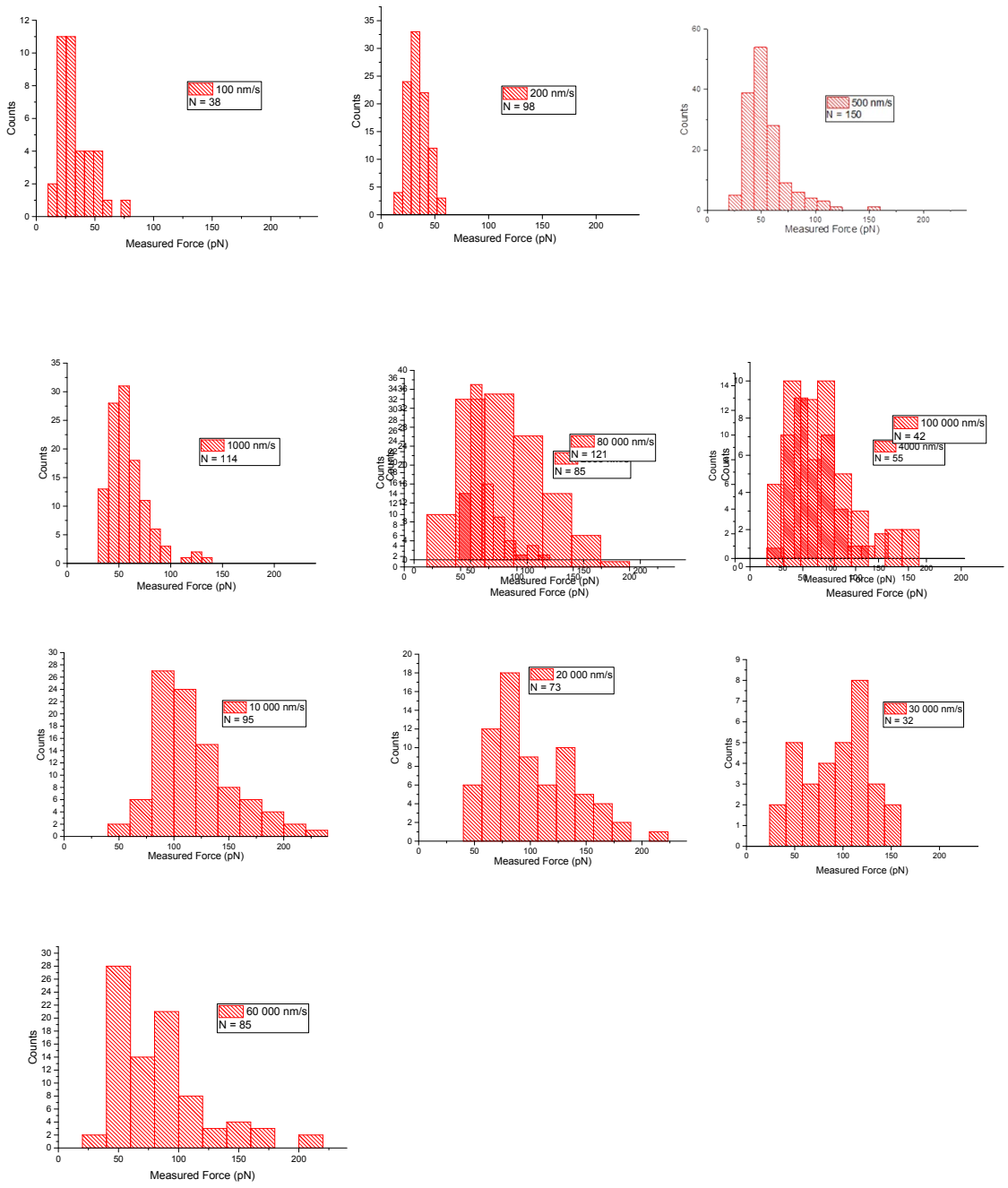

Figure S6. Force histograms of biotin-avidin bonds as a function of the pulling speed.

Supplementary Information References

1 C. K. Riener, C. M. Stroh, A. Ebner, C. Klampfl, A. A. Gall, C. Romanin, Y. L. Lyubchenko, P. Hinterdorfer, and H. J. Gruber, *Anal. Chim. Acta.,*2003, **479**, 59

2 S. Guo, C. Ray, A. Kirkpatrick, N. Lad, and B. B. Akhremitchev, *Biophys. J.*, 2008, **95**, 3964

3 R. De Paris, T. Strunz, K. Oroszlan, H.-J. Güntherodt, and M. Hegner, *Single Mol.*, 2000, **1**, 285

4 O. I. Vinogradova, H.-J. Butt, G. E. Yakubov, and F. Feuillebois, *Rev. Sci. Instrum*., 2001, **72**, 2330

5 H. Janovjak, J. Struckmeier, and D. J. Müller, *Eur. Biophys. J*., 2005, **34**, 91

6 C. A. Amo and R. Garcia, *ACS Nano*, 2016, **10**, 7117

7 G. I. Bell, *Science*, 1978, **200**, 618

8 E. Evans and K. Ritchie*, Biophys. J*., 1997, **72**, 1541